



Feng, S., & Vardanega, P. J. (2019). A database of saturated hydraulic conductivity of fine-grained soils: probability density functions. *Georisk: Assessment and Management of Risk for Engineered Systems and Geohazards*, 13(4), 255-261.
<https://doi.org/10.1080/17499518.2019.1652919>

Peer reviewed version

Link to published version (if available):
[10.1080/17499518.2019.1652919](https://doi.org/10.1080/17499518.2019.1652919)

[Link to publication record in Explore Bristol Research](#)
PDF-document

This is the author accepted manuscript (AAM). The final published version (version of record) is available online via Taylor & Francis at <https://www.tandfonline.com/doi/full/10.1080/17499518.2019.1652919> . Please refer to any applicable terms of use of the publisher.

University of Bristol - Explore Bristol Research

General rights

This document is made available in accordance with publisher policies. Please cite only the published version using the reference above. Full terms of use are available:
<http://www.bristol.ac.uk/red/research-policy/pure/user-guides/ebr-terms/>

A database of saturated hydraulic conductivity of fine-grained soils: probability density functions

Shuyin Feng^a and Paul J. Vardanega^{a*}

^a Department of Civil Engineering, University of Bristol, Bristol, United Kingdom

** Department of Civil Engineering, University of Bristol, University Walk, Bristol
BS8 1TR, United Kingdom. E-mail: p.j.vardanega@bristol.ac.uk*

A database of saturated hydraulic conductivity of fine-grained soils: probability density functions

Abstract: Saturated hydraulic conductivity is a key soil mechanics parameter which has widespread use in many geotechnical applications. In order to set up stochastic analyses, geotechnical modellers require databases to calibrate the parameter ranges and distributions employed. This paper uses a recently compiled database of saturated hydraulic conductivity measurements called FG/KSAT-1358 and reports on the fitting of various probability density functions to the data of void ratio, liquid limit, water content ratio and negative natural logarithm of k_{sat} . It is shown that the best fit distribution is the lognormal for void ratio, while the loglogistic distribution is most favoured for liquid limit and water content ratio, and the best fit distribution for $-\ln[k_{sat}(\text{m/s})]$ is the logistic function. The data of $-\ln[k_{sat}(\text{m/s})]$ is then subdivided according to liquid limit level, silt or clay classification, type of hydraulic conductivity test used and sample preparation/condition. When some subdivisions of the database are analysed, the best fit distribution is more variable with GEV and logistic being the most favoured for most of the studied subsets.

Keywords: saturated hydraulic conductivity; probability density functions; Akaike information criterion; corrected Akaike information criterion

1. Introduction

1.1. Saturated hydraulic conductivity

Saturated hydraulic conductivity (k_{sat}) is of key importance in many geotechnical designs (e.g., slopes, waste disposal facilities, road construction and foundation design). The ability to model potential variations in saturated hydraulic conductivity is important for those wishing to perform stochastic modelling of e.g., slopes in the humid tropics (Almedia et al. 2017; Shepherd et al. 2018). To select parameter ranges and distributions for use in such modelling geo-databases are needed. Geo-databases are commonly employed in geotechnics to make a-priori assessments of more complex

parameters from more readily obtainable ones (e.g., Kulhawy and Mayne, 1990).

There are many empirical and semi-empirical approaches in the literature to model saturated hydraulic conductivity, e.g., ‘Hazen’ (Hazen, 1893; 1895; 1911); the ‘Kozeny-Carman’ (Kozeny, 1927; Carman 1937; 1939; 1956). The difference between Hazen style approaches and ‘Kozeny-Carman’ style approaches is that the latter allows for variations of void ratio to be modelled (cf. Carrier, 2003) while Hazen relies on selection of an effective particle size. Zhai et al. (2018) adopted the “pore-size distribution function” method which gave good prediction for k_{sat} of sandy materials. Feng et al. (2019a, 2019b) show that the entire particle size distribution (PSD) curve can be used along with the Grading Entropy concept (e.g., Lörincz, 2005) to compute the normalized entropy co-ordinates which have also been demonstrated to predict k_{sat} reasonably well for gravel and sands. Both the ‘Hazen’ and ‘Kozeny-Carman’ approaches require calibration and therefore ‘transformation models’ (regression models) (cf. Phoon and Kulhawy, 1999a; 1999b) are needed.

1.2. FG-KSAT-1358

Feng and Vardanega (2019) have recently assembled a large database of 1358 k_{sat} measurements on a variety of fine-grained soils, hereafter referred to as FG/KSAT-1358 (full details of the sources and composition of the database can be found in Feng and Vardanega (2019) and are not repeated here for brevity). Using this large data-set and following the previous works of a transformation model has been proposed linking water content ratio (which is defined as the water content of the soil (w) normalized by the water content at the liquid limit (w_L) i.e. (w/w_L)). The water content ratio is equivalent to (e/e_L) for the fully saturated case. The transformation model developed in Feng and Vardanega (2019) follows that from previous works of Nagaraj (1993, 1994);

Sivapullaiah et al (2000); Mbonimpa et al. (2002) who proposed similar models linking k_{sat} with w/w_L but with smaller data-sets. The new model is calibrated with $n = 1352$ measurements in Feng and Vardanega (2019), and is given here as Equation (1):

$$\ln [k_{sat}(m/s)] = 4.083 \ln(w/w_L) - 20.074$$

$$[R^2 = 0.62, n = 1352, SE = 1.58, p < 0.0001] \quad (1a)$$

which can be re-arranged to:

$$k_{sat}(m/s) = 1.91 \times 10^{-9} (w/w_L)^{4.083} \quad (1b)$$

In this paper, FG-KSAT-1358 is used for a different purpose: to determine the best fit probability density functions that describe the key parameters within the database with associated goodness-of-fit tests. It should be noted that as six datapoints from FG/KSAT-1358 were identified as potential outliers and thus excluded in the calibration of the transformation model presented in Feng and Vardanega (2019): this data is also not considered in the analysis presented in this letter giving a dataset of $n = 1352$.

2. Probability Distributions in Geotechnical Engineering

Lumb (1966, 1970) examined the use of the normal, Gaussian and beta distributions for soil data-sets in Hong Kong. Rackwitz (2000) argued that a lognormal distribution had a ‘strong precedent’ in soils engineering. Vardanega and Bolton (2016) cautioned against the use the use of PDFs of soil parameters to examine the ULS state (as opposed to the SLS state), in part due to the well-known problem of lack of data at the tails. Scott et al. (2003) state “In geotechnical engineering, information about the mean and variance of a load or resistance is typically available, even though the exact distribution may not be known.” To remedy this problem geo-databases are needed. Arguably, fitted distributions calibrated with databases of soil parameters should be used to set up

stochastic and sensitivity analyses so that the range of potential outcomes for any particular geotechnical problem of interest can be better understood.

Recently Shepherd et al (2019) have shown in that Weibull distribution may better describe peak effective friction angle (ϕ'_{peak}) (number of datapoints (n) = 85) and cohesion intercept (c') (n = 86) for a database of soils from the island of Saint Lucia. While a lognormal distribution may be commonly used in geotechnical engineering (e.g., Rackwitz 2000; Scott et al. 2003), if a database is available then the engineer should investigate the applicability of a variety of statistical distributions.

3. FG/KSAT-1358: Probability Distributions

3.1. Analysis

The key parameters that describe FG/KSAT-1358 are the void ratio (e), the liquid limit (w_L), the water content ratio (w/w_L) (or e/e_L) and the negative natural logarithm of saturated hydraulic conductivity $-\ln[k_{sat}(\text{m/s})]$. It should be noted that the data of k_{sat} varies over seven orders of magnitude (see Table 1). Various probability density functions were fitted to each of these parameters in turn. The PDFs trialled were: ‘Weibull’ (W), ‘Normal’ (N); ‘Lognormal’ (LogN), ‘Exponential’ (Exp), ‘Generalized extreme value (GEV)’, ‘Logistic’ (Logi), ‘LogLogistic’ (LogLogi), ‘Gamma’ (G) (all fitted with functions available in Matlab®). As the ‘Normal’, ‘Generalized Extreme Value’ and ‘Logistic’ distributions can take negative values, in this work, they were not applied to the strictly positive parameters (e , w_L , w/w_L). However, the negative natural logarithm of saturated hydraulic conductivity $-\ln[k_{sat}(\text{m/s})]$ in this database is always positive for the studied database (FG/KSAT-1358), but theoretically it can still be negative. Therefore, for completeness, all the aforementioned eight probability distributions functions were trialled for $-\ln[k_{sat}(\text{m/s})]$. Figures 1(a), 2(a), 3(a) and 4(a)

shows the aforementioned distributions fitted to the data of ‘ e ’, ‘ w_L ’, ‘ w/w_L ’ and ‘ $-\ln[k_{sat}(m/s)]$ ’ respectively, the fitted parameters for the trialled probability distribution functions along with their general form can be found in Table S1 of the online supplement.

3.2. Goodness of fit tests

Table 2 shows the different distributions’ goodness of fit test results. In the analysis presented here both the Akaike Information Criterion (AIC) (Equation 2) (Akaike, 1974) and the Corrected Akaike Information Criterion (AIC_C) (Equation 3) which takes into account the size of the sample thus eliminate the risk of ‘over-fitting’ the data (e.g., Sugiura 1978; Hurvich and Tsai 1989; Hurvich and Tsai 1995; Burnham and Anderson, 2004) are given. The AIC and AIC_C can be expressed as:

$$AIC = -2 \log(L(\hat{\theta})) + 2K \quad (2)$$

$$AIC_C = -2 \log(L(\hat{\theta})) + 2K + \frac{2K(K+1)}{n-K-1} \quad (3)$$

where $L(\hat{\theta})$ is the likelihood function, K is the number of estimable parameters in the approximating model, while n is the sample size.

As the sample size here in this analysis is considerable ($n = 1352$), the computed results for AIC and AIC_C only differ in the decimal places (not shown here for brevity), the values quote in the subsequent analysis can be taken indicating that the AIC and AIC_C are essentially identical for the calculations presented in this paper. For the data of ‘ e ’ the best fit function is the lognormal, for ‘ w_L ’, ‘ w/w_L ’ the best fit distribution is the loglogistic, and for the data of ‘ $-\ln[k_{sat}(m/s)]$ ’ the best fit function is the logistic function, which is similar to a normal distribution but with larger tails (Birnbaum and Dudman 1963; Mudholkar and George 1978) therefore k_{sat} is essentially modelled with a

log-normal distribution. Figures 1(b), 2(b), 3(b) and 4(b) show the best fit distributions plotted for each of the four studied parameters.

4. PDFs for $-\ln[k_{sat}(\text{m/s})]$ database sub-sets

A PDF fitted to a parameter across the entire database may not be the best choice when the database is subdivided in certain ways. In Feng and Vardanega (2019) the effects on the transformation function were studied when FG-KSAT-1358 was split into four subcategories: liquid limit range (i.e. w_L greater than or less than 50%); position on the Casagrande chart (e.g., ASTM, 2017) (i.e. whether the material would classify as a clay or silt); permeability test method (i.e. falling head, constant head; flow pump or consolidation) and sample type would change the best fit PDF. For the sake of brevity only the effects of these sub-divisions on k_{sat} are shown in detail in this letter. It should be noted that for the two sub-categories: above and below the A-line $n = 1277$ points as 75 samples are without sufficient soil classification information (e.g. plasticity index). All the calculated AIC (AIC_C) of different PDF models for each sub-dataset are summarized in Table 3 with their fitted results presented in Figures S1-S10 in the online supplement.

4.1. Test method

Table 3 shows that for the ‘Falling head’; ‘Consolidation; ‘Flow pump’ and ‘Constant Head’ categories all suggest that the GEV is the best fit PDF.

4.2. Liquid limit level

For materials with $w_L \geq 50$ the normal distribution is favoured while for the $w_L < 50$ the Weibull distribution is favoured noting that in both cases the GEV ranked second.

4.3. Location with respect to the A-Line

For materials that would plot above the A-line the logistic distribution is favoured with loglogistic distribution ranking second and normal ranking third. For materials that would plot below the A-line the Gamma distribution is favoured with lognormal closely ranking second.

4.4. Sample type

For those samples classed as ‘disturbed’ or remoulded, which comprise most of the database, the Logistic function is favoured with normal distribution ranking second and loglogistic ranking third. For those samples classed as ‘undisturbed’ albeit potentially subjected to varying stress levels in the laboratory work the GEV distribution is favoured with the lognormal ranking second.

4.5. Comparison to the $n=1352$ dataset

As already mentioned, for the entire database for $-\ln(k_{sat})$ the logistic function is favoured with normal ranking second and loglogistic ranking third. From the above discussion it can be seen that the GEV and logistic features are either at the top or near the top of most of the rankings of the PDFs for each database subset.

5. Conclusions

The database FG-KSAT-1358 (Feng and Vardanega, 2019) has been analysed using probability density functions fitted to data or four key parameters: e , w_L , w/w_L and $-\ln[k_{sat}(m/s)]$. For e the lognormal distribution is top ranked PDF, while for w_L and w/w_L the loglogistic distribution was calculated to be the best fit based on examination of both the AIC and AICc. For the $-\ln[k_{sat}(m/s)]$ data the logistic function is the best fit. For the various subsets of $-\ln[k_{sat}(m/s)]$ examined: test method; liquid limit level;

location above or below the A-line and sample state generally the logistic and GEV distributions are the most favoured or ranked in the top three distributions of those studied in this letter. The results may be useful for those wishing to stochastically model variations of saturated hydraulic conductivity for various geotechnical applications.

Acknowledgments

The first author acknowledges the support from the China Scholarship Council (CSC) under the Grant CSC No. 201708060067. The authors thank Dr Flavia De Luca for her helpful comments and suggestions. The online supplement can be downloaded from the journal website.

Disclosure statement

The authors have no conflicts of interest to report.

Data availability statement

This research has not generated new experimental data.

References

- Akaike, H. 1974. "A new look at the statistical model identification." *IEEE Transactions Automatic Control*, 19(6), 716–723
- Almeida, S., Holcombe, E.A., Pianosi, F. and Wagener, T. 2017. "Dealing with deep uncertainties in landslide modelling for disaster risk reduction under climate change." *Natural Hazards and Earth System Science*, 17, 225-241.
- ASTM International. 2017. Standard Practice for Classification of Soils for Engineering Purposes (Unified Soil Classification System). West Conshohocken, United States.
- Birnbaum, A., and Dudman, J. 1963. "Logistic order statistics." *The Annals of Mathematical Statistics*, 658-663.
- Burnham, K.P. and Anderson, D.P. 2004. "Multimodal Inference: Understanding AIC and BIC in Model Selection." In: *Sociological Methods and Research*, 33(2), 261-304.

- Carman, P.C. 1937. "Fluid flow through granular beds." *Transactions-Institution of Chemical Engineers*, 15, 150-166.
- Carman, P.C. 1939. "Permeability of saturated sands, soils and clays." *The Journal of Agricultural Science*, 29(2), 262-273.
- Carman, P.C. 1956. *Flow of gases through porous media*, Butterworths Scientific Publications, London.
- Carrier III, W.D. 2003. "Goodbye, Hazen; Hello, Kozeny-Carman." *Journal of Geotechnical and Geoenvironmental Engineering*, 129(11), 1054-1056.
- Feng, S. and Vardanega, P.J. 2019. "Correlation of the hydraulic conductivity of fine-grained soils with water content ratio using a database." *Environmental Geotechnics*, <https://doi.org/10.1680/jenge.18.00166>
- Feng S., Vardanega P.J., Ibraim E. 2019a. "Comparison of Prediction Models for the Permeability of Granular Materials Using a Database." In: Hemeda S., Bouassida M. (eds) *Contemporary Issues in Soil Mechanics. GeoMEast 2018*. Sustainable Civil Infrastructures. Springer, Cham, pp. 1-13.
- Feng, S., Vardanega, P.J., Ibraim, E., Widyatmoko, I. and Ojum, C. 2019b. "Permeability assessment of some granular mixtures." *Géotechnique*, 69(7), 646-654
- Hazen, A. 1893. "Some physical properties of sand and gravels. Massachusetts State Board of Health." *24th Annual Report*. Wright & Potter Printing, Boston, USA.
- Hazen, A. 1895. *The filtration of public water-supplies*. John Wiley & Son, New York, USA.
- Hazen, A. 1911. "Discussion of 'Dam on Sand Foundation' by A. C. Koenig." *Transactions of American Society of Civil Engineers*, 73, 199-203.
- Hurvich, C.M. and Tsai, C-L. 1989. "Regression and time series model selection in small samples." *Biometrika*, 76(2), 297-307.
- Hurvich, C.M. and Tsai, C-L. 1995. "Model Selection for Extended Quasi-Likelihood Models in Small Samples." *Biometrics*, 51(3), 1077-1084.
- Kozeny, J. 1927. "Über kapillare Leitung des Wassers im Boden (Aufstieg, Versickerung und Anwendung auf die Bewässerung)." [in German.] *Sitzungsber. Akad. Wiss., Wien.*, 136(a), 271–306.
- Kulhawy, F. H. and Mayne, P. W. 1990. Manual on estimating soil properties for foundation design, *Report. No. EL-6800*, Electric Power Research Institute, Palo Alto, California, USA

- Lőrincz, J., Imre, E., Gálos, M., Trang, Q. P., Rajkai, K., Fityus, S., and Telekes, G. 2005. "Grading entropy variation due to soil crushing." *International Journal of Geomechanics*, 5(4), 311-319
- Lumb, P. 1966. "The variability of natural soils." *Canadian Geotechnical Journal*, 3(2), 74-97.
- Lumb, P. 1970. "Safety factors and the probability distribution of soil strength." *Canadian Geotechnical Journal*, 7(3), 225-242.
- Mbonimpa, M., Aubertin, M., Chapuis, R. and Busssière, B. 2002. "Practical pedotransfer functions for estimating the saturated hydraulic conductivity." *Geotechnical and Geological Engineering*, 20(3), 235-259
- Mudholkar, G. S., and George, E. O. 1978. "A remark on the shape of the logistic distribution." *Biometrika*, 65(3), 667-668.
- Nagaraj, T.S., Pandian, N.S., and Narashimha Raju, P.S.R. 1993. "Stress state-permeability relationships for fine-grained soils." *Géotechnique*, 43(2), 333-336
- Nagaraj, T.S., Pandian, N.S., and Narashimha Raju, P.S.R. 1994. "Stress state-permeability relations for overconsolidated clays." *Géotechnique*, 44(2), 349-352.
- Phoon, K-K. and Kulhawy, F. H. 1999a. "Characterization of Geotechnical Variability." *Canadian Geotechnical Journal*, 36(4), 612-624.
- Phoon, K-K. and Kulhawy, F. H. 1999b. "Evaluation of geotechnical property variability." *Canadian Geotechnical Journal*, 36(4), 625-639.
- Rackwitz, R. 2000. "Reviewing probabilistic soil modelling." *Computers and Geotechnics*, 26(3-4), 199-223.
- Scott, B., Kim, B. J. and Salgado, R. 2003. "Assessment of Current Load Factors for Use in Geotechnical Load and Resistance Factor Design." *Journal of Geotechnical and Geoenvironmental Engineering*, 129(4), 287-295.
- Shepherd, C. J., Vardanega, P. J., Holcombe, E. A. and Michaelides, K. 2018. "Analysis of design choices for a slope stability scenario in the humid tropics." *Proceedings of the Institution of Civil Engineers – Engineering Sustainability*, 171(1), 37-52.
- Shepherd, C.J., Vardanega, P.J., Holcombe, E.A., Hen-Jones, R. and De Luca, F. 2019. "Minding the geotechnical data gap: appraisal of friction angle variability for slope stability modelling in the Eastern Caribbean." *Bulletin of Engineering Geology and the Environment*, <http://dx.doi.org/10.1007/s10064-018-01451-5> (ahead of print)

- Sivapullaiah, P.V, Sridharan, A., and Stalin, V.K. 2000. "Hydraulic conductivity of bentonite-sand mixtures." *Canadian Geotechnical Journal*, 37(2): 406–413.
- Sugiura, N. 1978. "Further analysts of the data by Akaike' s information criterion and the finite corrections." *Communications in Statistics - Theory and Methods*, 7(1), 13-26
- Vardanega, P. J. and Bolton, M. D. 2016. "Design of Geostructural Systems." *ASCE-ASME Journal of Risk and Uncertainty in Engineering Systems, Part A: Civil Engineering*, 2(1), 04015017.
- Zhai Q., Rahardjo H. and Satyanaga, A. (2018) "A pore-size distribution function based method for estimation of hydraulic properties of sandy soils." *Engineering Geology* 246: 288-292.

Table 1. Summary statistics for FG/KSAT-1358 (SD = standard deviation; COV = coefficient of variation) ($n = 1352$)

Table 2. AIC and AICc for the fitted distributions shown in Figures 1-4 (strongest fits shown in bold type).

Table 3. AIC and AICc for the fitted distributions to the $-\ln[k_{sat}(\text{m/s})]$ data when split by liquid limit level, silt or clay classification, type of hydraulic conductivity test used and sample preparation/condition (strongest fits shown in bold type).

Figure 1. (a) Different PDFs fitted to the void ratio data from FG-KSAT-1358; (b) Best fit PDF (lognormal) shown

Figure 2. (a) Different PDFs fitted to the w_L data from FG-KSAT-1358; (b) Best fit PDF (loglogistic) shown

Figure 3. (a) Different PDFs fitted to the w/w_L data from FG-KSAT-1358; (b) Best fit PDF (loglogistic) shown

Figure 4. (a) Different PDFs fitted to the $-\ln[k_{sat}(\text{m/s})]$ data from FG-KSAT-1358; (b) Best fit PDF (logistic) shown

Table 1. Summary statistics for FG/KSAT-1358 (SD = standard deviation; COV = coefficient of variation) ($n = 1352$)

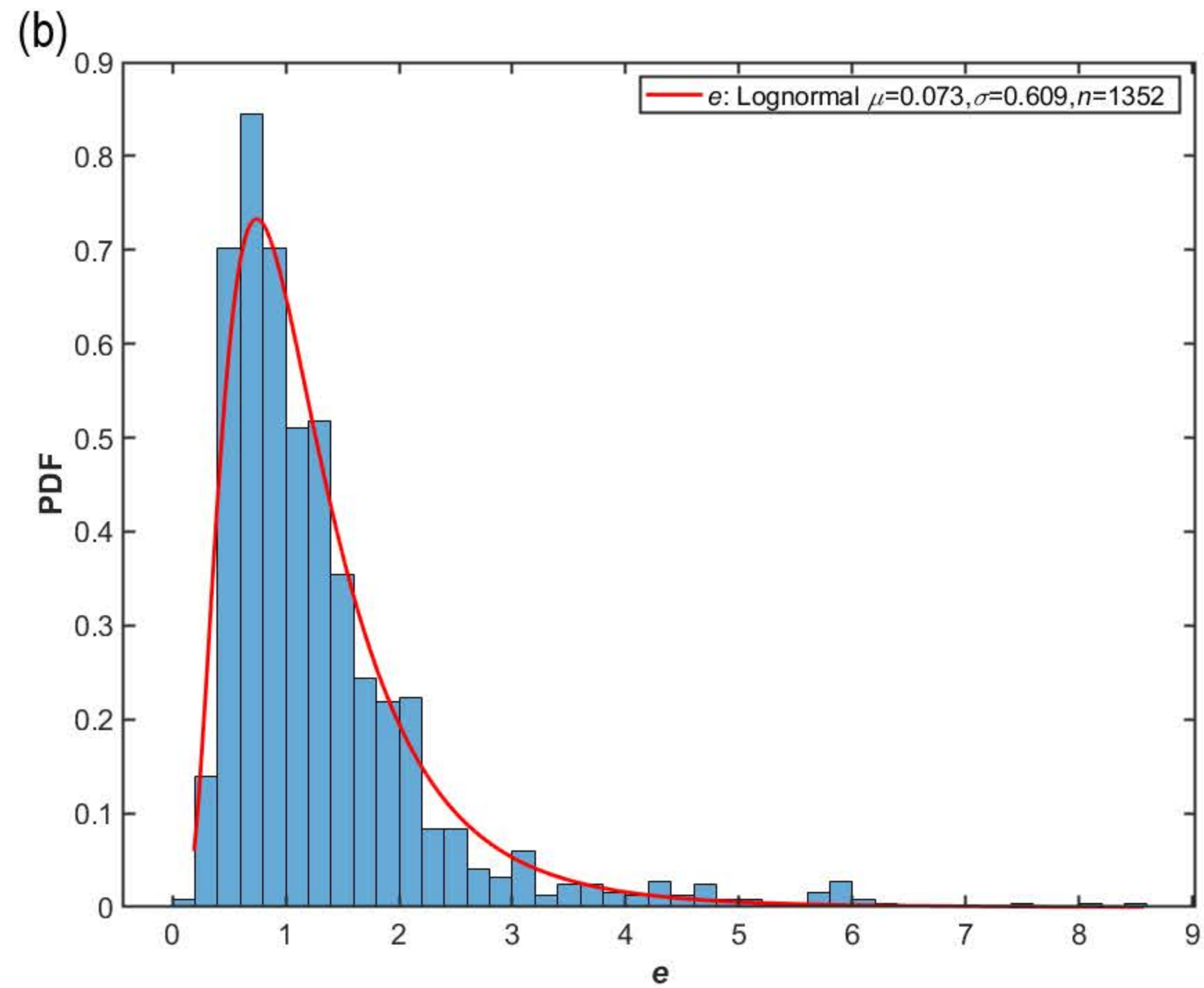
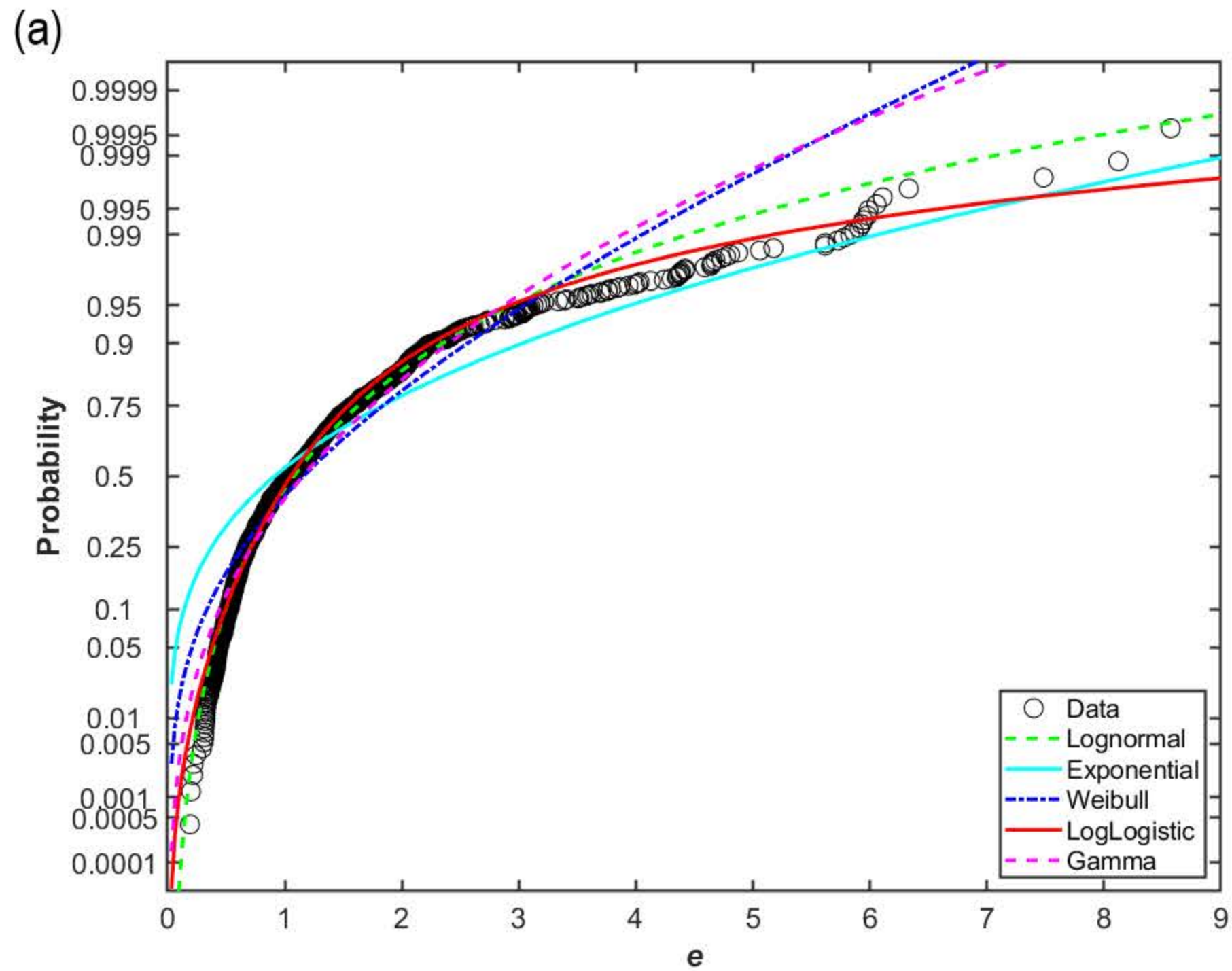
Parameter	Min.	Max.	Mean	SD	COV
e	0.19	8.57	1.32	1.01	0.76
w_L (%)	22	675	84.84	83.09	0.98
w/w_L	0.058	2.99	0.69	0.35	0.51
k_{sat} (m/s)	1.44×10^{-13}	7.50×10^{-6}	2.21×10^{-8}	2.73×10^{-7}	12.38
$-\ln[k_{sat}$ (m/s)]	11.80	29.57	22.04	2.55	0.12

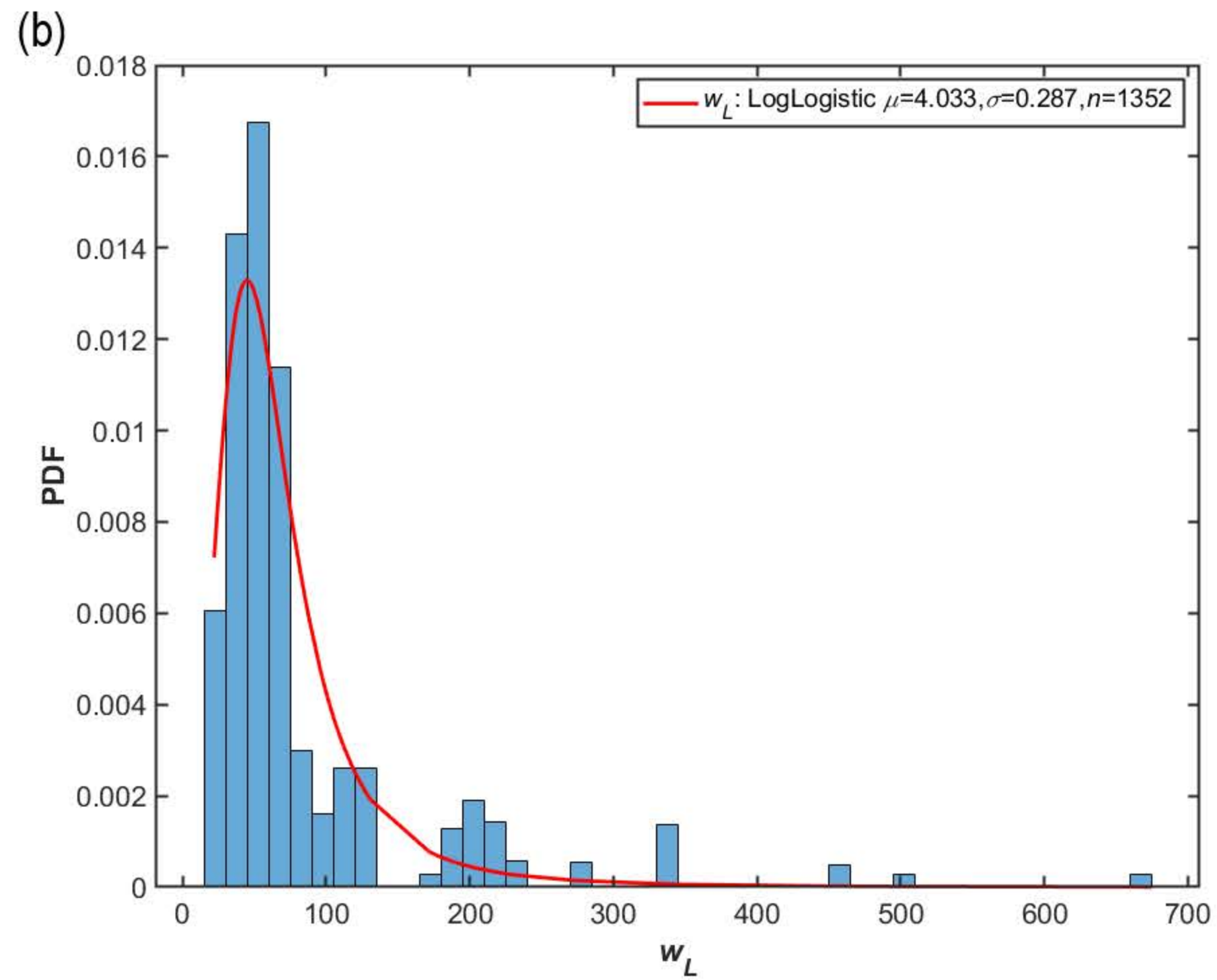
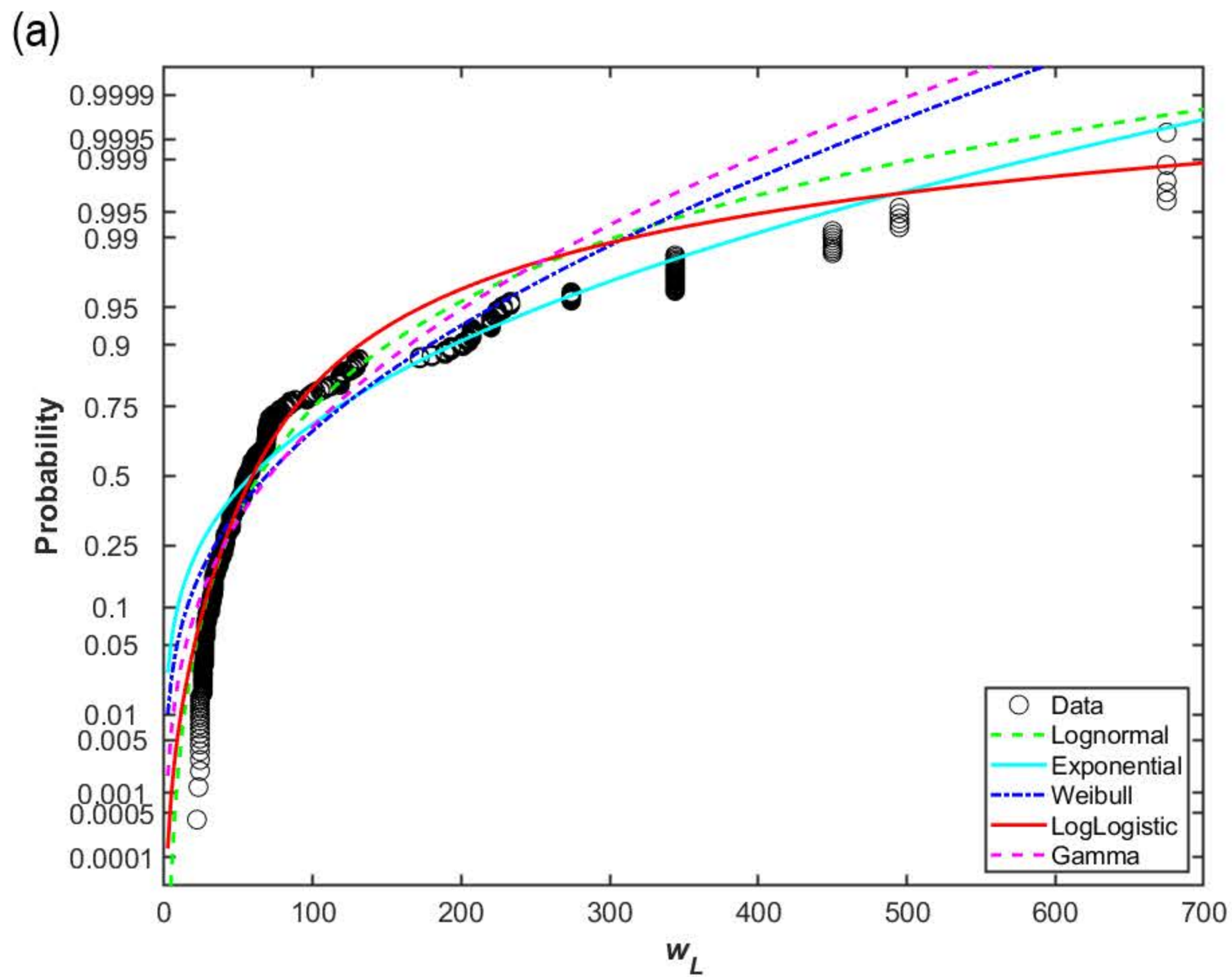
Table 2. AIC and AICc for the fitted distributions shown in Figures 1-4 (strongest fits shown in bold type).

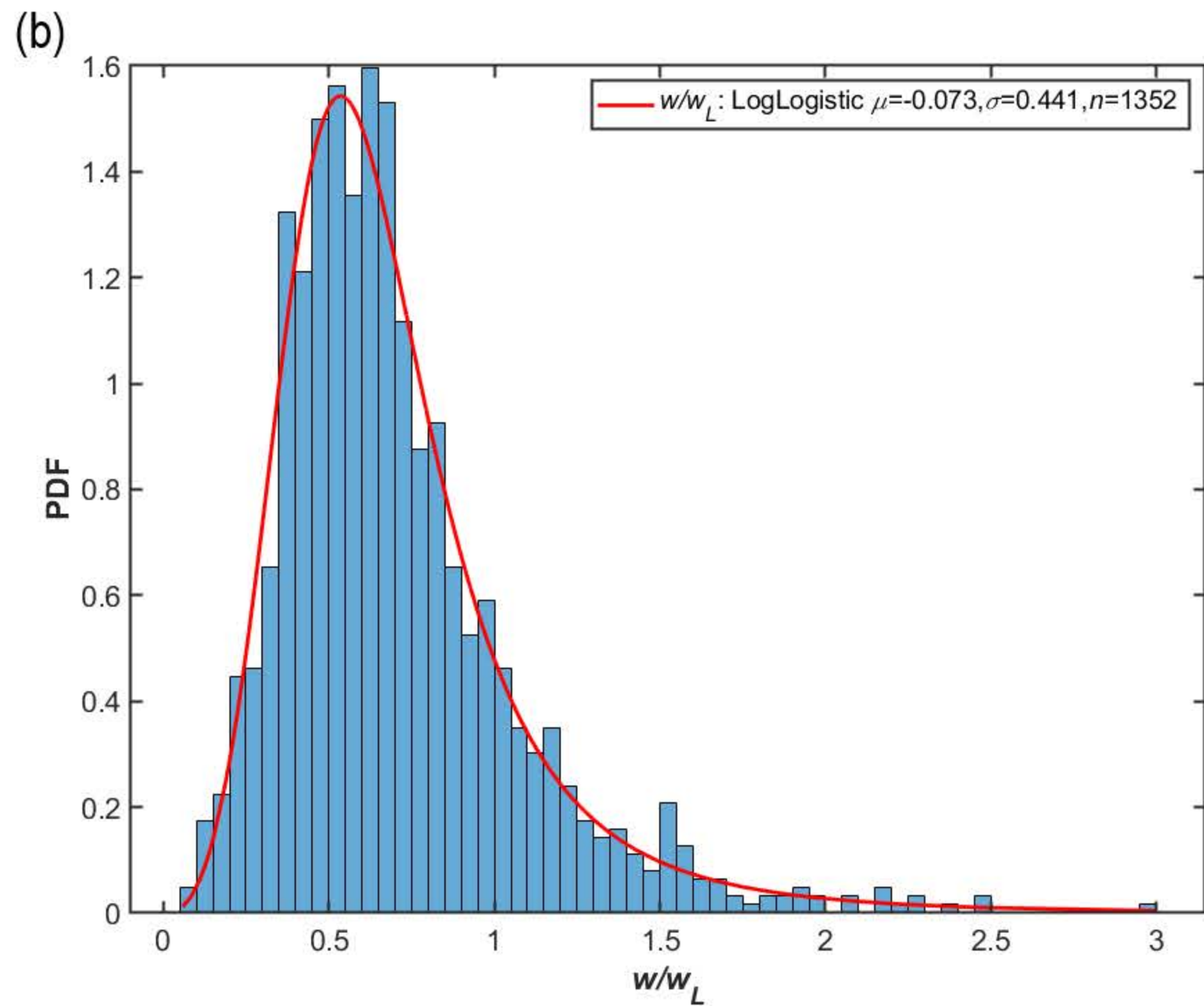
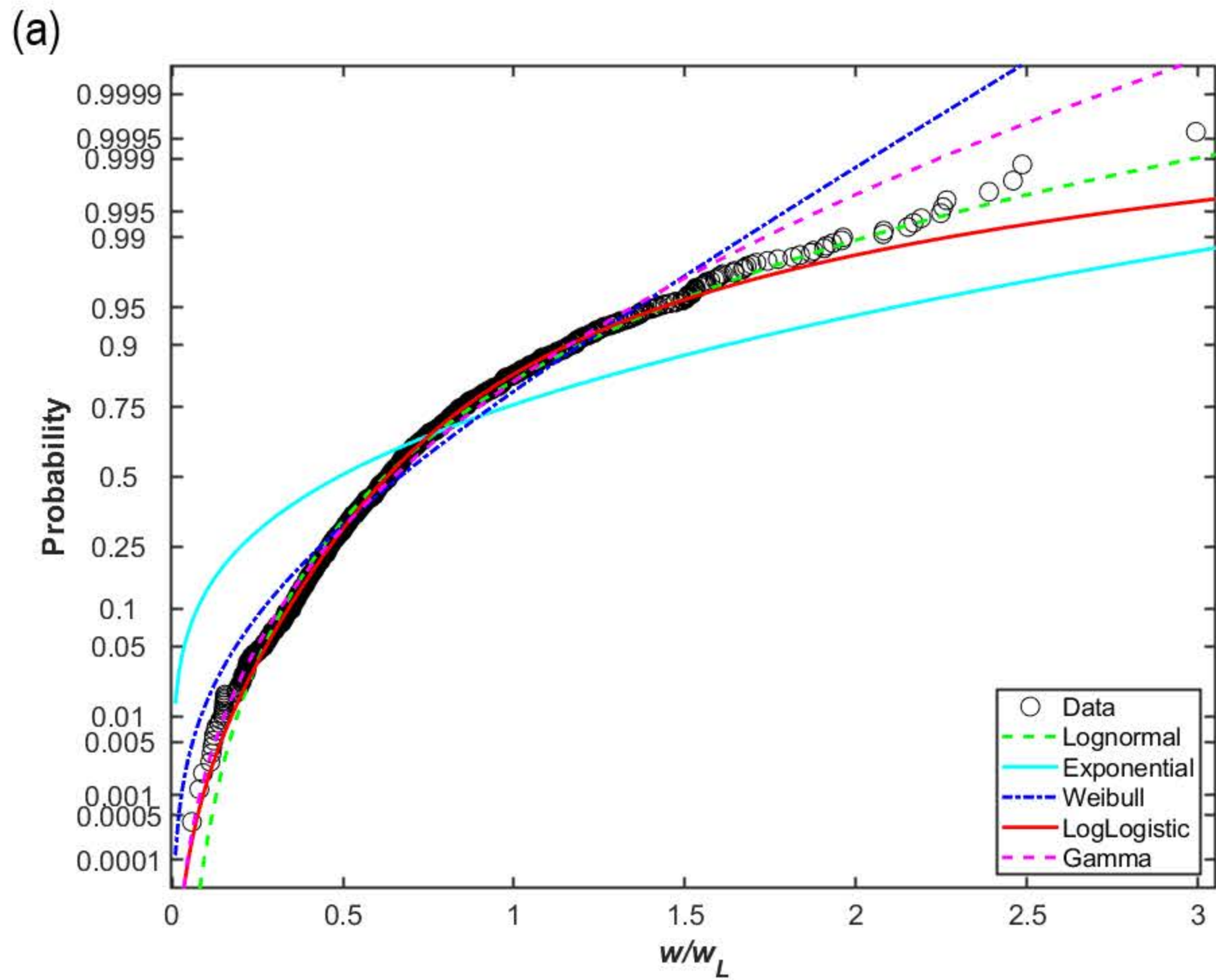
	AIC or AIC _c							
	N	Exp	LogN.	W	GEV	Logi.	LogLogi.	G
e	-	3197	2500	2855	-	-	2516	2686
w_L (%)	-	13635	12981	13516	-	-	12936	13364
w/w_L	-	1627	670	788	-	-	631	663
$-\ln[k_{sat} \text{ (m/s)}]$	5965	10258	6041	6020	5994	5946	5983	6008

Table 3. AIC and AICc for the fitted distributions to the $-\ln[k_{sat}(\text{m/s})]$ data when split by liquid limit level, silt or clay classification, type of hydraulic conductivity test used and sample preparation/condition (strongest fits shown in bold type).

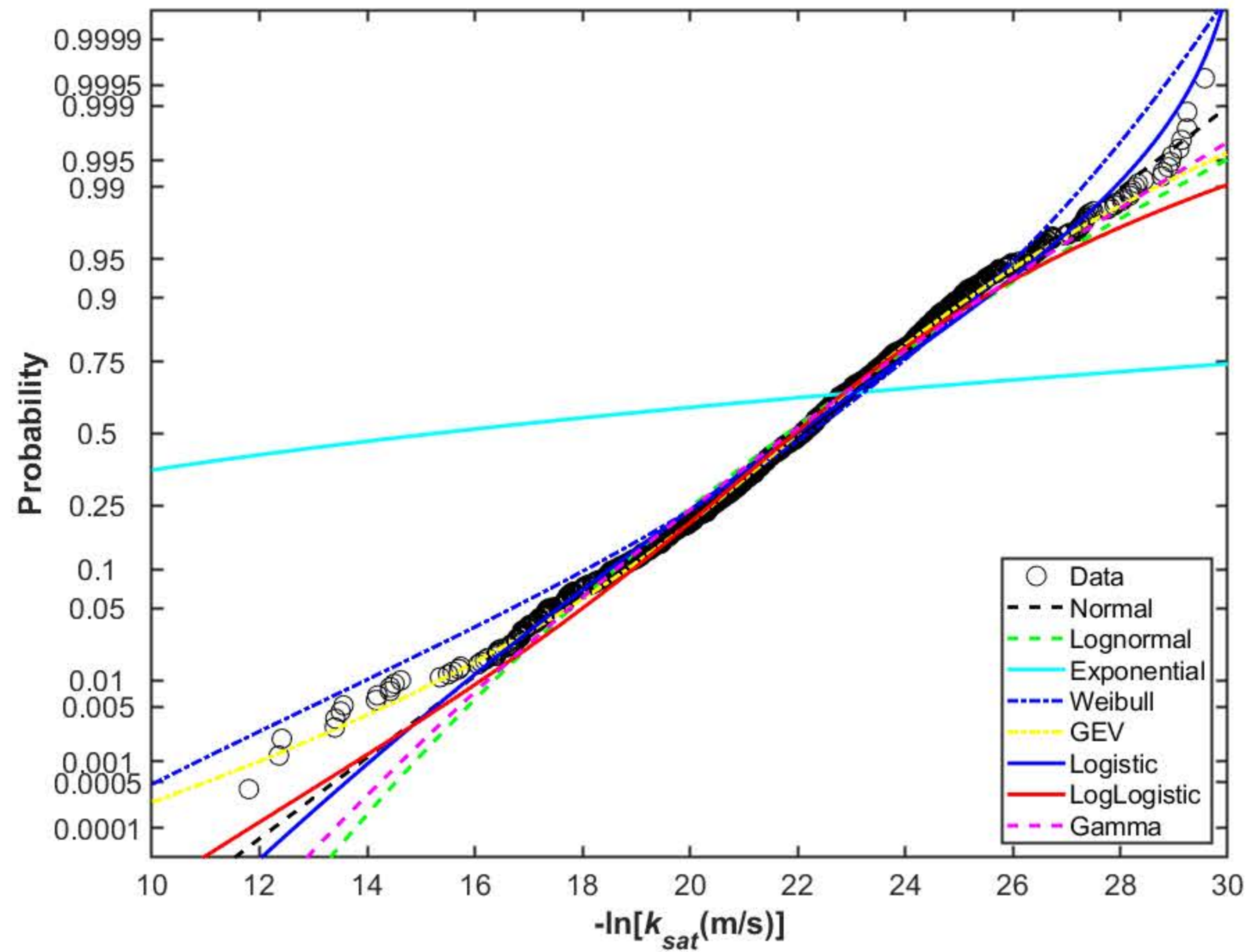
$-\ln[k_{sat}(\text{m/s})]$	n	AIC or AIC _c								Figure in supplement
		N	Exp	LogN	W	GEV	Logi	LogLogi	G	
Falling head	580	2692	4706	2768	2620	2603	2685	2727	2740	S1
Consolidation	512	2299	4238	2284	2383	2283	2302	2291	2288	S2
Flow pump	91	474	749	478	471	470	481	484	476	S3
Constant head	169	748	1379	754	745	741	757	762	752	S4
$w_L \geq 50\%$	854	3919	7044	3932	3991	3925	3929	3935	3924	S5
$w_L < 50\%$	498	2288	4025	2355	2217	2220	2282	2320	2330	S6
Above A-line	934	4289	7680	4356	4346	4324	4245	4269	4327	S7
Below A-line	343	1614	2771	1611	1648	1612	1628	1626	1610	S8
Disturbed	1103	5235	9044	5309	5275	5260	5214	5251	5277	S9
Undisturbed	127	509	1038	503	535	493	514	509	505	S10



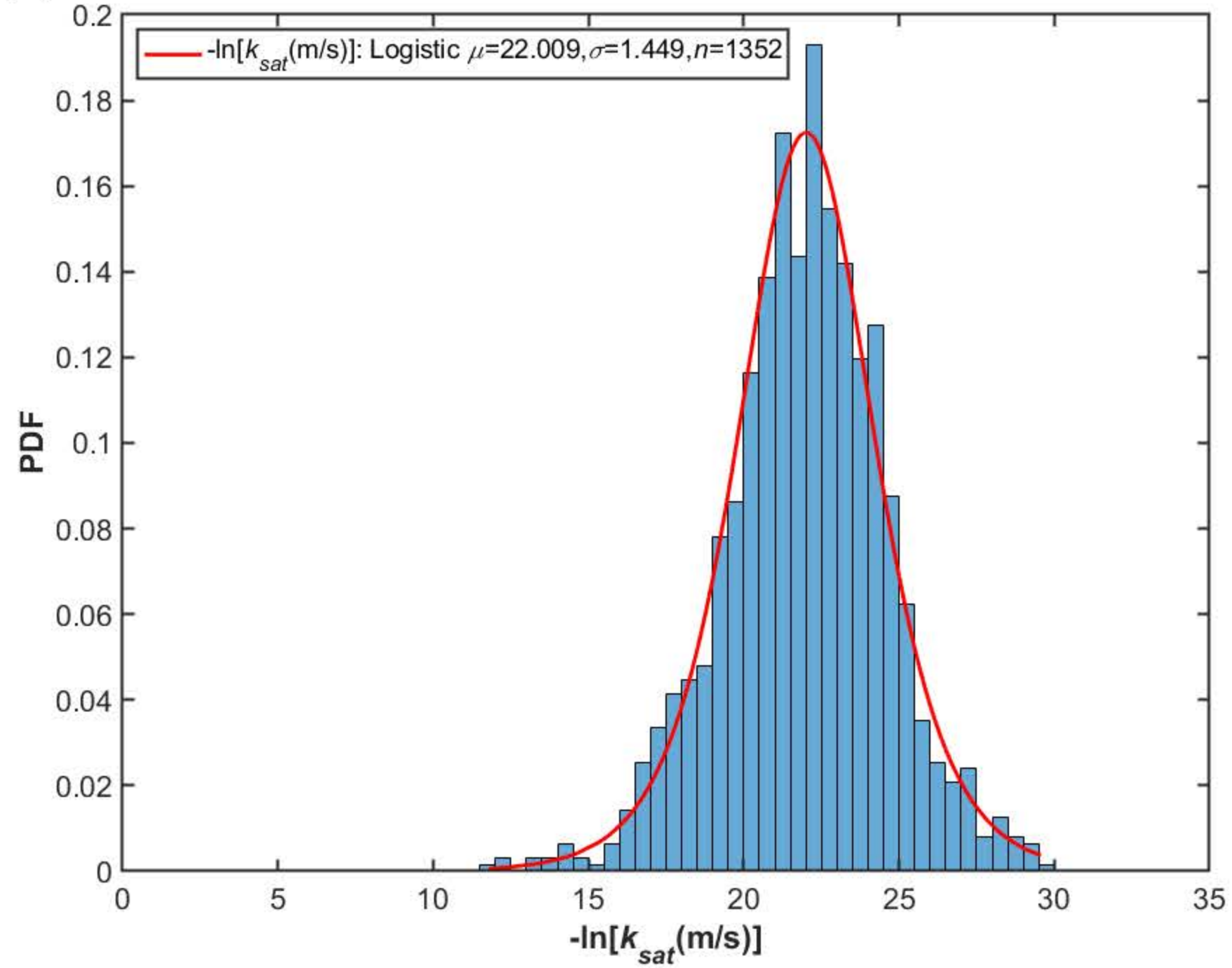




(a)



(b)



ONLINE SUPPLEMENT

Table S1. Fitted parameters of different probability density function for e , w_L , w/w_L and $-\ln[k_{sat}(\text{m/s})]$ using the database (FG/KSAT-1358) (6 potential outliers removed, $n = 1352$).

General form (notation follows MathWorks® 2019)		n	Parameters	e	w_L	w/w_L	$-\ln[k_{sat}(\text{m/s})]$
Normal	$f(x \mu, \sigma) = \frac{1}{\sigma\sqrt{2\pi}} e^{-\frac{(x-\mu)^2}{2\sigma^2}}$	2	μ mean	-	-	-	21.96
			σ standard deviation	-	-	-	2.61
Exponential	$f(x \mu) = \frac{1}{\mu} e^{-\frac{x}{\mu}}$	1	μ mean	1.32	84.44	0.73	21.96
Lognormal	$f(x \mu, \sigma) = \frac{1}{x\sigma\sqrt{2\pi}} e^{-\frac{(\log x - \mu)^2}{2\sigma^2}}$	2	μ mean of logarithmic values	0.07	4.16	-0.48	3.08
			σ standard deviation of logarithmic values	0.61	0.67	0.51	0.12
Weibull	$f(x a, b) = \frac{b}{a} \left(\frac{x}{a}\right)^{b-1} e^{-(x/a)^b}$	2	a scale parameter	1.47	92.03	0.80	23.10
			b shape parameter	1.51	1.26	2.05	9.15
GEV	for $k \neq 0$: $f(x k, \mu, \sigma) = \left(\frac{1}{\sigma}\right) \exp\left(-\left(1 + k \frac{(x-\mu)}{\sigma}\right)^{-\frac{1}{k}}\right) \left(1 + k \frac{(x-\mu)}{\sigma}\right)^{-1-\frac{1}{k}}$ for $k = 0$: $f(x 0, \mu, \sigma) = \left(\frac{1}{\sigma}\right) \exp\left(-\exp\left(-\frac{(x-\mu)}{\sigma}\right)\right) - \frac{(x-\mu)}{\sigma}$	3	k shape parameter	-	-	-	-0.29
			σ scale parameter	-	-	-	2.70
			μ location parameter	-	-	-	21.05
Logistic	$f(x \mu, \sigma) = \frac{\exp\left\{\frac{x-\mu}{\sigma}\right\}}{\sigma(1 + \exp\left\{\frac{x-\mu}{\sigma}\right\})^2}$	2	μ mean	-	-	-	22.01
			σ scale parameter	-	-	-	1.45
LogLogistic	$f(x \mu, \sigma) = \frac{e^z}{\sigma x(1 + e^z)^2}$ where $z = \frac{\log(x) - \mu}{\sigma}$	2	μ mean of logarithmic values	0.05	4.08	-0.46	3.09
			σ scale parameter of logarithmic values	0.35	0.36	0.28	0.07
Gamma	$f(x a, b) = \frac{1}{b^a \Gamma(a)} x^{a-1} e^{-\frac{x}{b}}$	2	a shape parameter	2.64	1.95	4.22	67.97
			b shape parameter	0.50	43.22	0.17	0.32

Ref: MathWorks® (2019) <https://uk.mathworks.com/help/stats/prob.normaldistribution.pdf.html>. Accessed 14 June, 2019

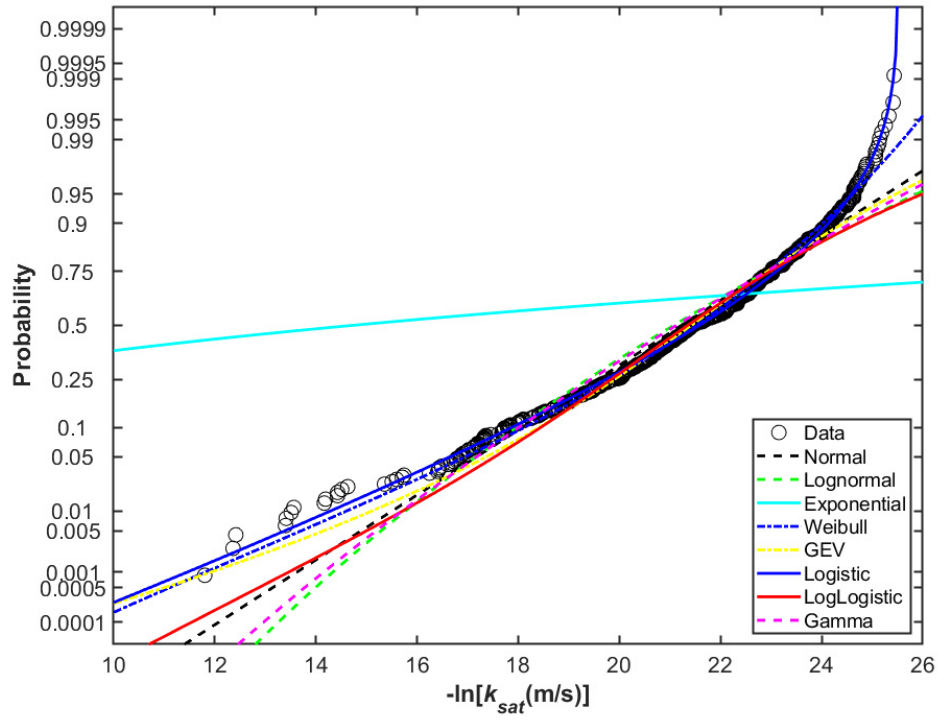


Figure S1. Different PDFs fitted to the $-\ln[k_{sat}(\text{m/s})]$ data from data subset: falling head

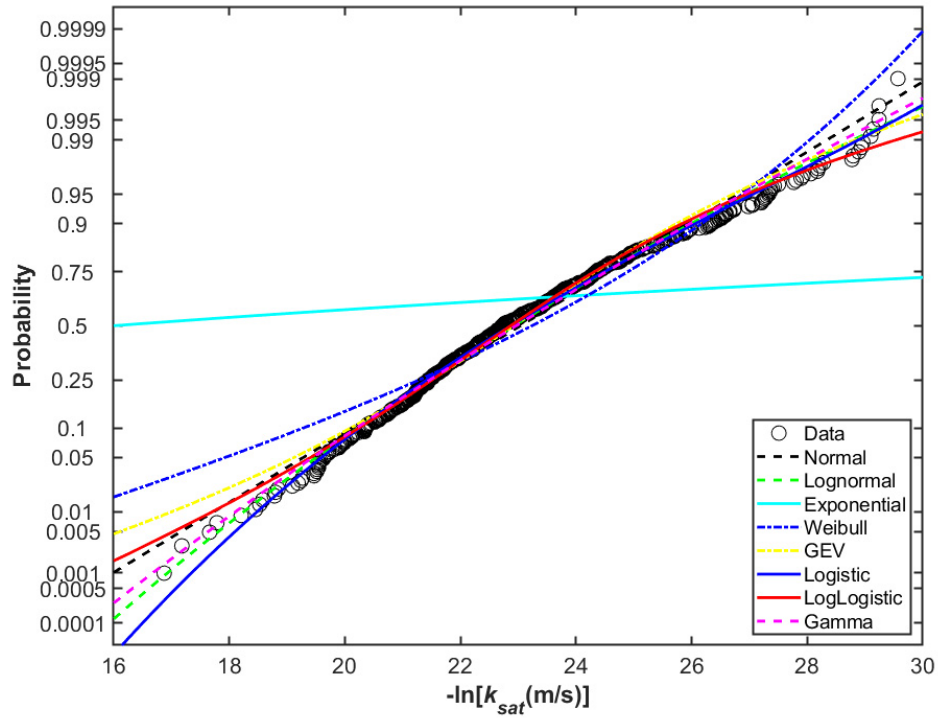


Figure S2. Different PDFs fitted to the $-\ln[k_{sat}(\text{m/s})]$ data from data subset: consolidation

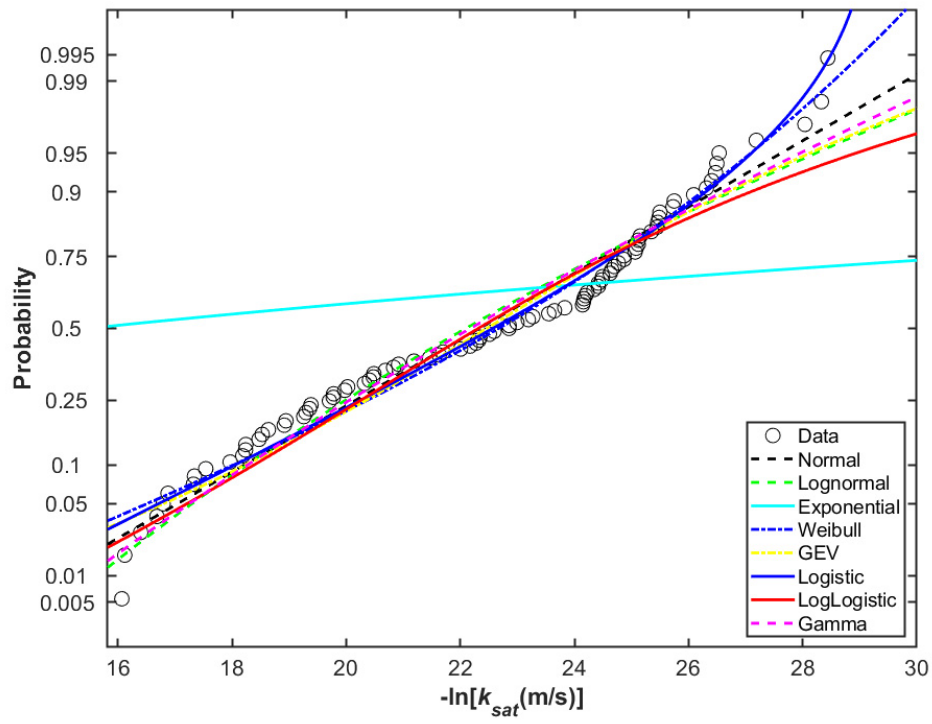


Figure S3. Different PDFs fitted to the $-\ln[k_{sat} \text{ (m/s)}]$ data from data subset: flow pump

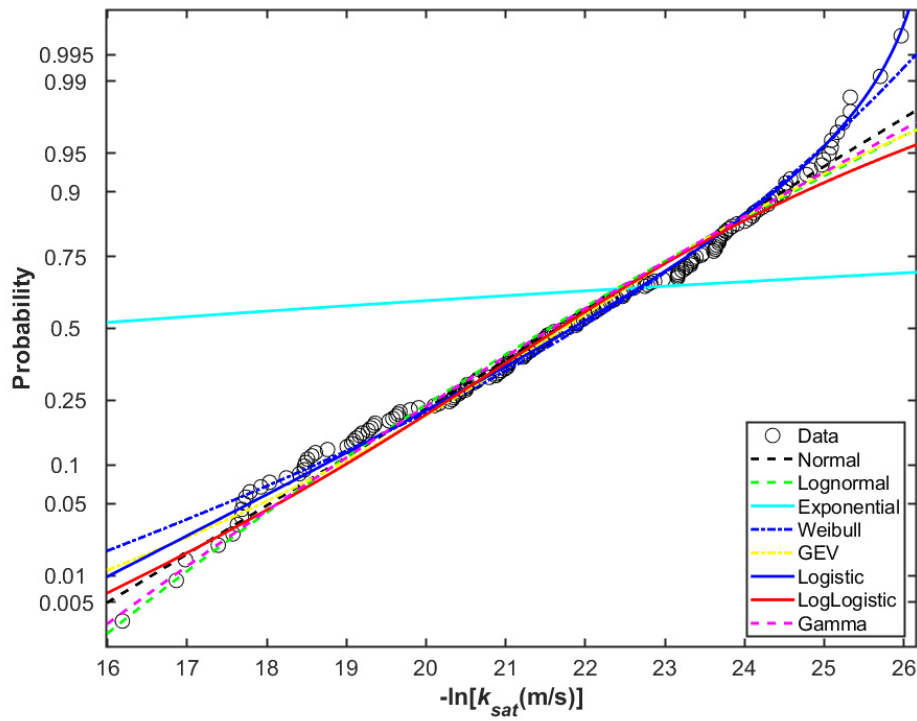


Figure S4. Different PDFs fitted to the $-\ln[k_{sat} \text{ (m/s)}]$ data from data subset: constant head

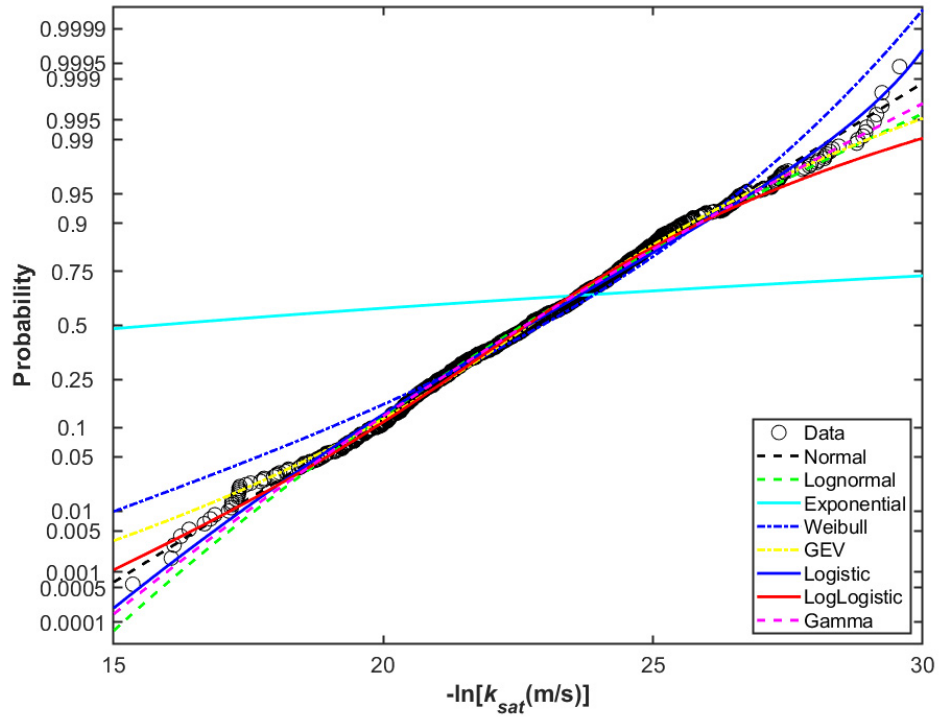


Figure S5. Different PDFs fitted to the $-\ln[k_{sat}(\text{m/s})]$ data from data subset: $w_L \geq 50\%$

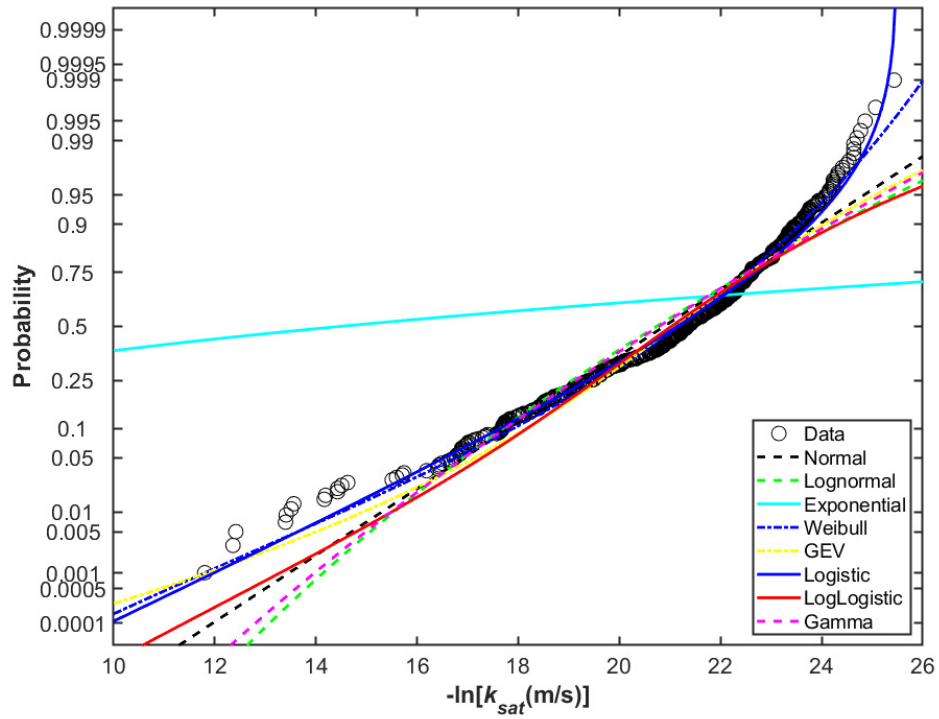


Figure S6. Different PDFs fitted to the $-\ln[k_{sat}(\text{m/s})]$ data from data subset: $w_L < 50\%$

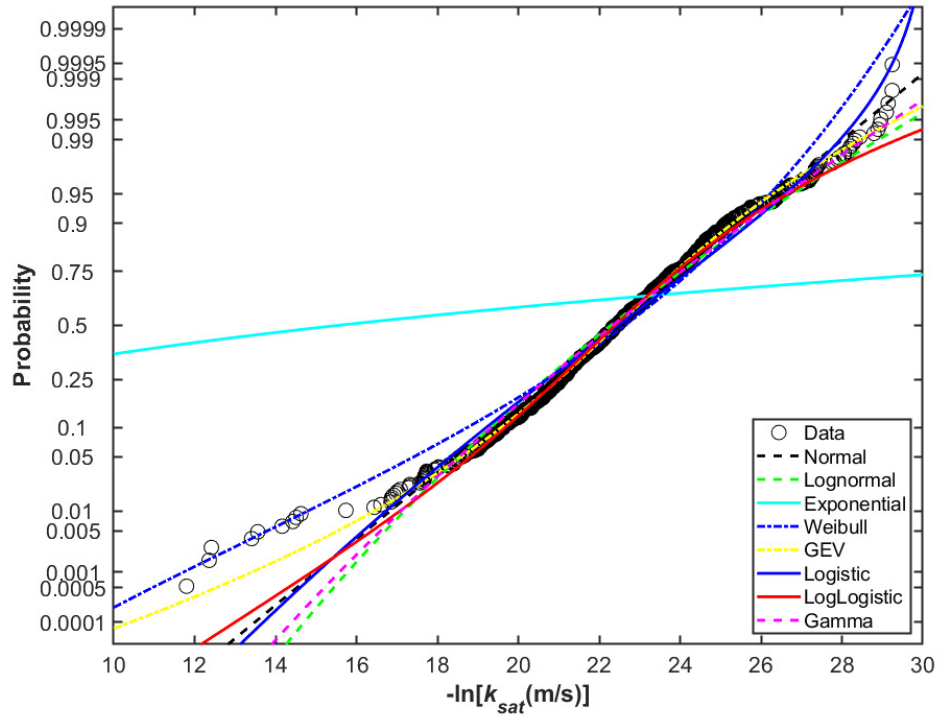


Figure S7. Different PDFs fitted to the $-\ln[k_{sat} \text{ (m/s)}]$ data from data subset: above A line

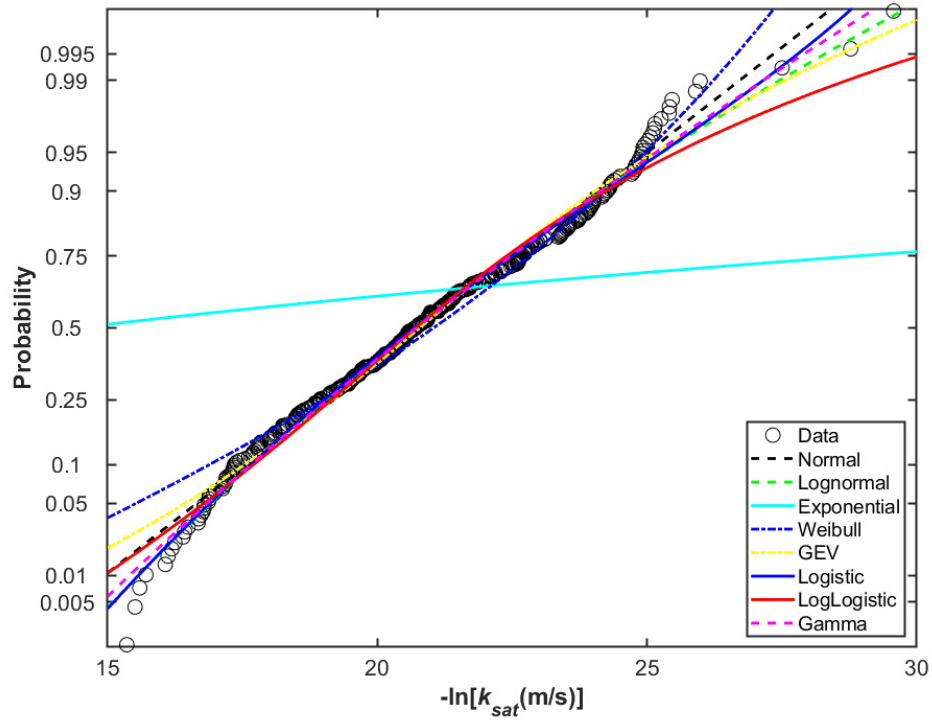


Figure S8. Different PDFs fitted to the $-\ln[k_{sat} \text{ (m/s)}]$ data from data subset: below A line

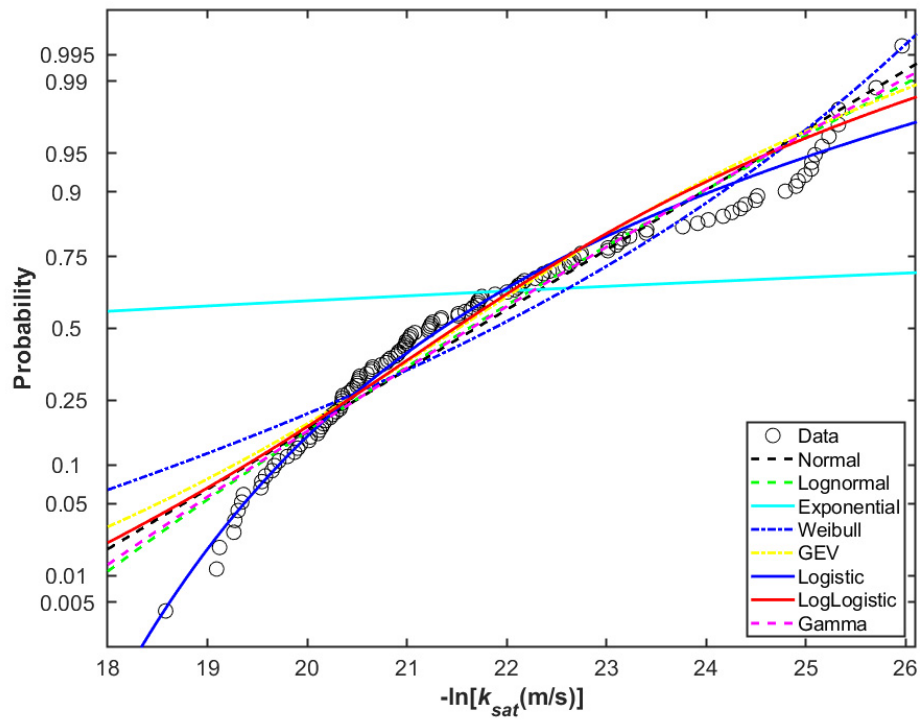


Figure S9. Different PDFs fitted to the $-\ln[k_{sat}(\text{m/s})]$ data from data subset: disturbed

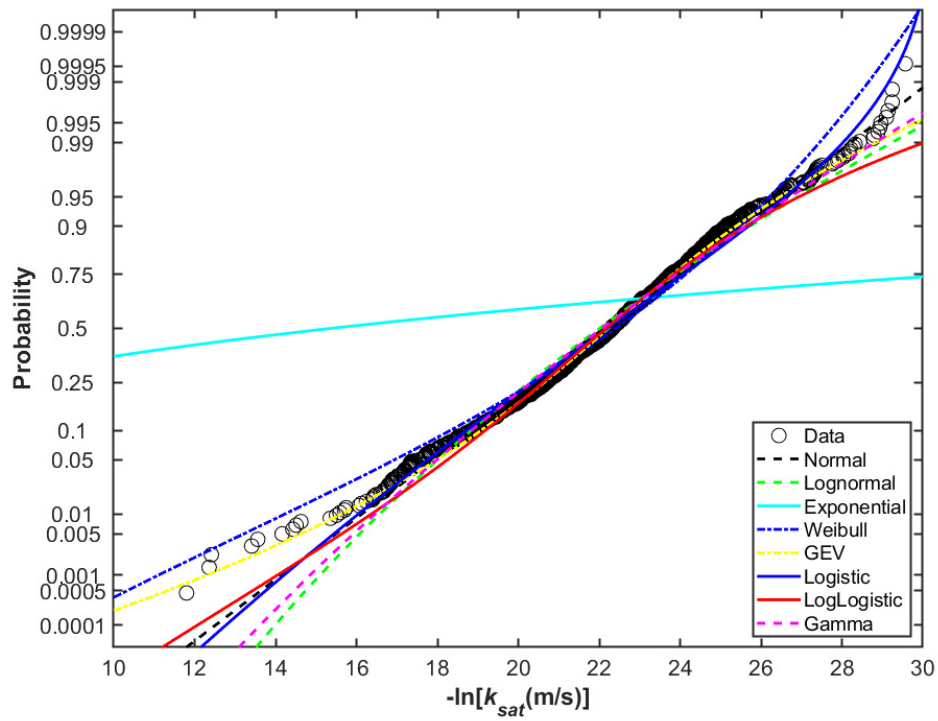


Figure S10. Different PDFs fitted to the $-\ln[k_{sat}(\text{m/s})]$ data from data subset: undisturbed